



EMORY
LIBRARIES &
INFORMATION
TECHNOLOGY

OpenEmory

The Involvement of Autophagy Pathway in Exaggerated Ischemic Brain Damage in Diabetic Mice

Ning Wei, *Nanjing University*
[Shan Ping Yu](#), *Emory University*
Xiao-Huan Gu, *Emory University*
Dong-Dong Chen, *Emory University*
[Matthew Whalin](#), *Emory University*
Ge-Lin Xu, *Nanjing University*
Xin-Feng Liu, *Nanjing University*
[Ling Wei](#), *Emory University*

Journal Title: CNS Neuroscience and Therapeutics

Volume: Volume 19, Number 10

Publisher: Wiley Open Access | 2013-10-01, Pages 753-763

Type of Work: Article | Final Publisher PDF

Publisher DOI: 10.1111/cns.12123

Permanent URL: <https://pid.emory.edu/ark:/25593/ts4cb>

Final published version: <http://dx.doi.org/10.1111/cns.12123>

Copyright information:

© 2013 John Wiley & Sons Ltd.

This is an Open Access work distributed under the terms of the Creative Commons Attribution 4.0 International License (<https://creativecommons.org/licenses/by/4.0/>).

Accessed April 22, 2025 3:28 PM EDT

The Involvement of Autophagy Pathway in Exaggerated Ischemic Brain Damage in Diabetic Mice

Ning Wei,^{1,2} Shan-Ping Yu,² Xiao-Huan Gu,² Dong-Dong Chen,² Matthew K. Whalin,² Ge-Lin Xu,¹ Xin-Feng Liu¹ & Ling Wei^{2,3}

1 Department of Neurology, Nanjing University School of Medicine, Jinling Hospital, Nanjing, China

2 Department of Anesthesiology, Emory University School of Medicine, Atlanta, GA, USA

3 Department of Neurology, Emory University School of Medicine, Atlanta, GA, USA

Keywords

Autophagy; Blood–brain barrier; Cell death; Diabetes; Ischemic stroke.

Correspondence

Ling Wei, M.D., Department of Anesthesiology, Emory University School of Medicine, Atlanta, 101 Woodruff Circle, Suite 630, GA 30322, USA.

Tel.: +1-404-718-8661;

Fax: +1-404-717-6300;

E-mail: lwei7@emory.edu

or

Xinfeng Liu, M.D., Ph.D., Department of Neurology, Nanjing University School of Medicine, Jinling Hospital, 305 East Zhongshan Road, Nanjing, 210002, Jiangsu Province, China

Tel.: +86-25-8537-2631;

Fax: +86-25-8480-1861;

E-mail: xfliu2@gmail.com

Received 11 January 2013; revision 3 April

2013; accepted 7 April 2013

SUMMARY

Background: Patients with Diabetes are at greater risk for ischemic stroke and usually suffer more severe ischemic brain damage than nondiabetic patients. However, the underlying mechanism of the exaggerated injury is not well defined. **Aims:** Macroautophagy (hereafter called autophagy in this report) plays a key role in cellular homeostasis and may contribute to cell death as well. Our aim was to determine whether autophagy was involved in the enhanced susceptibility of diabetic brain cells to ischemic injury and explore it as a possible target for the treatment of stroke in a diabetic condition. **Results:** A type II diabetic mouse model generated by combined administration of streptozotocin and nicotinamide showed enlarged infarct volume, increased cell death and excessive blood–brain barrier (BBB) disruption compared with nondiabetic stroke mice. After ischemic stroke, both diabetic and nondiabetic mice showed enhanced autophagosome formation and autophagic flux as demonstrated by increased expression of autophagy signals Beclin 1, microtubule-associated protein light-chain II (LC3-II), and decreased autophagy-specific substrate p62. The increased autophagic activity was significantly higher in diabetic stroke mice than that in nondiabetic stroke mice. The autophagy inhibitor 3-methyladenine (3-MA) attenuated the exaggerated brain injury and improved functional recovery. **Conclusions:** These data suggest that autophagy contributes to exacerbated brain injury in diabetic condition, and autophagy-mediated cell death may be a therapeutic target in diabetic stroke.

doi: 10.1111/cns.12123

Introduction

Focal cerebral ischemia is one of the leading causes of death and disability worldwide, and more than 30% of stroke patients are known to be diabetic [1,2]. More than 90% of the 200 million patients with diabetes across the world are type 2 diabetes, which is characterized by high blood glucose in the context of insulin resistance and relative insulin deficiency. It is well known that both acute hyperglycemia and chronic diabetes exaggerate ischemic brain damage in experimental and clinical stroke, but the mechanisms remain elusive [3–5]. Brain lactic acid accumulation and tissue acidosis due to hyperglycemia have been most commonly correlated with more extensive tissue damage in diabetic stroke [6]. Nevertheless, rapid correction of the hyperglycemia

after acute ischemia with reduced brain lactic acid level has not improved outcomes in clinical trials [6,7]. In addition to the vascular and hyperglycemic alterations, other mechanisms might contribute to the enhanced susceptibility of the diabetic brain to ischemic injury [1,8].

Autophagy is a physiological process long known to maintain cellular homeostasis through lysosomal degradation, recycling long-lived proteins and eliminating damaged organelles such as mitochondria and endoplasmic reticulum. Autophagy is thus known primarily as a prosurvival mechanism for cells facing nutrient deprivation or other stress conditions. However, accumulating evidence indicates that autophagy can contribute to cell death processes under pathological conditions [9–12]. The double-edged effect of autophagy on pancreatic β -cell loss in diabetes

and in cerebral ischemia has been implicated [12–14]. The functional role of autophagy in the pathogenesis of diabetic complications such as atherosclerosis, cardiomyopathy, nephropathy, and neuropathy is currently under intensive investigation [15–17].

In studies of nondiabetic animals, autophagic activities increase following cerebral ischemia [10,18–20], and some evidence indicates that the autophagy pathway could contribute to ischemia-mediated neuronal cell death [18,21–23]. Information about autophagy in diabetic stroke animals has been very limited. Two recent reports showed that 23 days after transient common carotid artery (CCA) occlusion seemingly mimicking a global ischemic insult, increased neuronal loss, astrocytes activation, $A\beta$ generation, and autophagy activity were observed in the hippocampus of diabetic mice [17,24]. On the other hand, to our knowledge, there has been no study to investigate the involvement of autophagic pathway in the pathogenesis of exaggerating acute brain damage after focal ischemic stroke in diabetic animals.

The present investigation examined the autophagic activity in a murine type 2 diabetic stroke model. We further examined a possible treatment of diabetic stroke using an autophagy inhibitor 3-methyladenine (3-MA) and determine the role of autophagy in the pathogenesis of ischemic brain damage in diabetic mice.

Materials and Methods

Diabetic Mouse Model

All animal experiments and surgical procedures were approved by the Institutional Animal Care and Use Committee at Emory University and met NIH standards. Adult male C57BL/6 mice (National Cancer Institute, NCI, Bethesda, MD, USA), 10–12 weeks old and approximately 25 g in weight, were used in this study. Diabetes was induced by i.p. injection of nicotinamide (210 mg/kg; Sigma, St. Louis, MO, USA) dissolved in saline 15 min before an i.p. administration of streptozotocin (180 mg/kg; Sigma) dissolved in citrate buffer (pH 4.5; Sigma) prepared immediately before use [25,26]. Controls received the vehicles of both substances. After treatment with STZ or vehicle, animals were housed for 2 months and given food and water ad libitum. Blood glucose levels following a four-hour fast were monitored twice per month using samples from the tail vein with the FreeStyle[®] glucose meter (Abbott Diabetes Care, Alameda, CA, USA). Two months after the induction of diabetes, blood was collected from orbit. Twenty-five microlitres of plasma were assayed for insulin by ELISA using a Mercodia Ultra-sensitive Insulin ELISA Kit (Mercodia AB Uppsala, Sweden).

Focal Cerebral Ischemic Stroke Model

The focal cerebral ischemic stroke in adult male mice was induced as previously described [27]. Briefly, animals were anesthetized with i.p. injection of 4% chloral hydrate. Focal ischemia restricted to the right barrel/sensorimotor cortex was induced by permanent occlusion of 2–3 distal branches of the MCA. This was accompanied by 7-min bilateral CCA ligation. Sham animals were done with the same surgery procedure without MCA or CCA occlusion. During surgery and recovery periods, body temperature was monitored using a rectal probe and maintained at 37.0 ± 0.5 °C using a heating pad and a temperature-controlled, ventilated incubator.

3-Methyladenine Administration

3-Methyladenine (3-MA; Sigma), a widely used pharmacological inhibitor of autophagy, was prepared to a final concentration of 30 mg/mL in 2 μ L saline and was administered by intracerebroventricular (i.c.v.) injection immediately after ischemia onset into the ipsilateral ventricle. Saline alone injection served as a negative control.

Infarct Volume Assessment

At 24 h after stroke, the brain was removed and sliced into 1-mm coronal sections using a mouse brain matrix and incubated in 2% 2, 3,5-triphenyl-tetrazolium chloride solution at 37 °C for 5 min. Brain sections were scanned, and the unstained versus stained area was determined using NIH Image J on the ventral side of six brain slides per animal. The infarct area (mm^2) of staining in each slice was multiplied by the slice thickness (1 mm) to get the infarct volume (mm^3). The indirect infarct volume was calculated by the difference between the volume of contralateral cortex and the volume of the TTC-stained portion (nonischemic) of ipsilateral cortex of each mouse, following the calculation: contralateral volume – (ipsilateral volume – infarct volume). This method helps to correct edema in the ipsilateral hemisphere in order to achieve accurate assessments of infarct volume. The brain infarct volume was the summation of six individual section volumes.

Terminal Deoxynucleotidyl Transferase Biotin-dUPT Nick End Labeling

Ten μ m brain sections were prepared every 90 μ m across the region of interest. Cell death was assessed using the Terminal deoxynucleotidyl transferase biotin-dUPT nick end labeling (TUNEL) staining kit according to the manufacturer's instructions (Dead-End Fluorometric TUNEL system; Promega, Madison, WI, USA). The slides were counterstained with Hoechst 33342 (1:20,000; Life Technologies, Grand Island, NY, USA) for 5 min to reveal the nucleus of all cells before mounting with ProLong Antifade mounting medium (Life Technologies). The result was presented as ratio of TUNEL-positive cells among all nuclei within 400 \times magnification fields.

Immunohistochemical Staining

Brain cryosections (10 μ m thickness) were fixed with 4% paraformaldehyde for 15 min, permeabilized with 0.2% Triton X-100 for 5 min, and blocked with 1% fish gelatin (Sigma) for 1 h at room temperature. Specimens were then incubated with the following primary antibodies overnight at 4 °C: goat anticollagen type IV (1:400; Millipore, Billerica, MA, USA), rabbit anti-LC3 (microtubule-associated protein 1A light-chain 3; 1:400; Cell Signaling, Danvers, MA, USA), goat anticalthepsin D (1:200; Santa Cruz Biotechnology, Santa Cruz, CA, USA) and anti-Beclin 1 (1:5000; Abcam, Cambridge, MA, USA). For the staining of occludin, brain cryosections were fixed with ethanol at 4°C for 30 min followed by ice-cold acetone for 3 min, washed, blocked, and incubated with mouse antioccludin (1:100; Life Technologies). After rinsing with PBS, brain sections were then treated for 1 h at room tem-

perature with the relevant secondary antibodies: Cy5-conjugated donkey anti-goat IgG, Cy3-conjugated donkey anti-rabbit IgG (Jackson ImmunoResearch, West Grove, PA, USA) or Alexa Fluor 488 anti-rabbit IgG and anti-mouse IgG (1:200; Life Technologies). Slides were mounted with ProLong Antifade mounting medium (Life Technologies) and analyzed under a fluorescent microscope (BX51; Olympus, Tokyo, Japan).

Cell Counting

For systematic random sampling in design-based stereological cell counting, every ninth brain section (90 μm apart) across the entire region of interest was counted. For multistage random sampling, six fields per brain section were randomly chosen in the penumbra region [27] under 400 \times magnification of a fluorescent microscope. This was repeated in six separate sections per brain.

Western Blotting

Twenty-four hours after ischemia, 3–5 animals for each group were used to collect ipsilateral penumbra tissue samples. The brain tissues were lysed using modified radioimmunoprecipitation assay buffer (50 mmol/L HEPES, pH 7.3, 1% sodium deoxycholate, 1% Triton X-100, 0.1% sodium dodecylsulfate, 150 mmol/L NaCl, 1 mmol/L ethylenediaminetetraacetic acid, 1 mmol/L Na_3VO_4 , 1 mmol/L NaF), and protease inhibitor cocktail (Sigma) for 30 min, followed by centrifugation at 17,000 g for 15 min. Protein concentration of each sample was determined using the bicinchoninic acid assay (Sigma). Samples of 20 μg proteins were electrophoresed on a 6% to 20% sodium dodecyl sulfate–polyacrylamide gradient gel in a Hoefer Mini-Gel system (Amersham Biosciences, Piscataway, NJ, USA) and transferred in the Hoefer Transfer Tank (Amersham Biosciences) to a polyvinylidene difluoride membrane (BioRad, Hercules, CA). Membranes were blocked with buffer (Tris-buffered saline containing 0.1% Tween-20, pH 7.6%, 5% bovine serum albumin) and then incubated with one of the following antibodies overnight at 4°C: rabbit anti-LC3 (1:1000; Novus, Littleton, CO, USA), anti-SQSTM1/A170/p62, rabbit (1:500; Wako Inc., Osaka, Japan), rabbit anti-Bcl-2 (1:1000; Cell Signaling), rabbit anticlaved caspase-3 (1:500; Cell Signaling) and mouse antioccludin (1:500; Life Technologies). Mouse β -actin (Sigma) was used as the protein loading control. The blots were washed in 0.5% Tris-buffered saline containing 0.1% Tween-20 (TBST) and incubated with alkaline phosphatase-conjugated anti-rabbit or anti-mouse IgG (Promega) for 2 hrs at room temperature. Finally, membranes were washed with TBST followed by three washes with Tris-buffered saline. Signal was detected by the addition of 5-bromo-4-chloro-3-indolyl-phosphate/nitroblue tetrazolium (BCIP/NBT) solution (Sigma). Data were quantified and analyzed using the NIH image J program (NIH, Bethesda, MD, USA). The expression level of each protein was corrected against the loading control of β -actin.

Evaluation of Neurological Deficits

The adhesive-removal test is a sensitive test for assessing sensorimotor deficits after focal cerebral ischemia affecting the sensorimotor cortex [18,28]. This was used to evaluate the neurological dysfunction

after stroke, as previously described [18]. Briefly, a training session (for 3 days, 1–2 trials per day) was performed until the mice could take off the sticky dots on their paws within 12 seconds before surgical procedures. Animals were tested before and 23 h after ischemia by an investigator who was blinded to the experimental groups. The shortest time (tested from 4 to 5 trials) required to sense (time to detect) and remove (time to remove) the sticky dot from the left paw was recorded. All testing trials were conducted during the day time.

Statistical Analysis

Two-tailed Student's *t*-test was used for comparison of two experimental groups. Multiple comparisons were performed using one-way analysis of variance followed by Tukey's test for multiple comparisons. For pairwise comparisons, one-way analysis followed by Bonferroni selective comparisons were performed. Changes were identified as significant if *P* was less than 0.05. Data were expressed as mean \pm SEM.

Results

Pathophysiological Assessments of the Experimental Diabetic Mouse

A diabetic animal model was created in adult male mice via injection of streptozotocin and nicotinamide (STZ/NA). Within 2 months after the induction, animals exhibited significantly lower body weight and elevated levels of blood glucose (200–300 mg/dL) with respect to age-matched vehicle control mice (Table 1). This hyperglycemia was stable during the 2-month period before ischemic surgery. Plasma insulin levels, measured 2 months after STZ/NA treatment, were decreased by 68% in diabetic mice as compared with controls. Treatment with the autophagy inhibitor 3-MA (30 mg/mL in 2 μL saline, i.c.v. injection) had no effect on these variables in diabetic mice before and during 24-hr period after ischemia. The mortality rate after stroke surgery in diabetes group was seemingly higher, yet not significant different from nondiabetic stroke animals.

Increased Autophagosome Formation in Diabetic Stroke Mice

To study autophagy after ischemic stroke, diabetic and nondiabetic animals were subjected to a focal ischemic insult targeting the right barrel/sensorimotor cortex [27]. Beclin 1 is an essential autophagy protein known to activate the lipid kinase Vps34 and induce autophagy [29]. Immunostaining showed that the

Table 1 General features of the experimental diabetic mouse models

Measurements	Nondiabetic	Diabetic	Diabetic + 3-MA
Body weight (g)	30.4 \pm 0.6	23.0 \pm 0.7*	24.0 \pm 0.7*
Blood glucose (mg/dL)	112 \pm 6	279 \pm 19*	275 \pm 17*
Serum insulin ($\mu\text{g/L}$)	0.74 \pm 0.15	0.25 \pm 0.05*	0.24 \pm 0.04*
N	16	11	11

Values are the mean \pm SEM. 3-MA, 3-Methyladenine. **P* < 0.05 vs. nondiabetes controls.

increase in brain beclin 1 expression in diabetic stroke mice was significantly greater than that in nondiabetic stroke animals at 12 and 24 h after stroke (Figure 1).

A cytosolic form of microtubule-associated protein light-chain I (LC3-I) is lipidated during autophagy to form LC3-II, a widely used marker for autophagosome [21,30,31]. To evaluate whether the autophagy pathway is involved in the diabetic ischemic brain, immunostaining of LC3 was visualized by fluorescence microscopy as punctuate structures representing autophagosomes 24 hrs after ischemic insult (Figure 2A–C and Figure 3A–C). On the other hand, diffuse staining of LC3 could be intermittently detected in the sham control brain (Figure 2A). The LC3-positive cells were primarily located in the penumbra region of the brain after focal ischemia. The percentage of cells with bright LC3 puncta

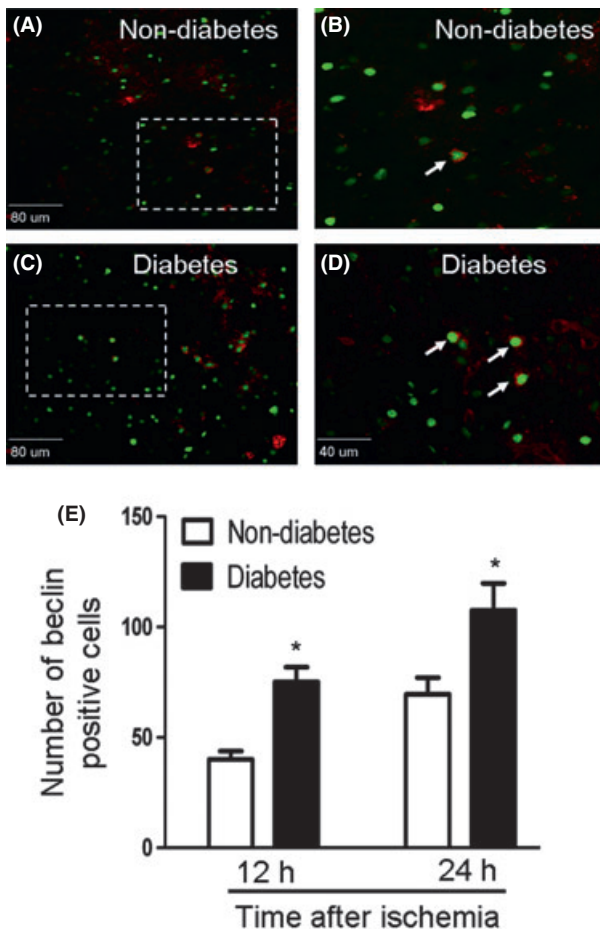


Figure 1 Increased autophagosome after cerebral ischemia in diabetic mice. Immunohistochemical staining of brain sections from stroke animals, focusing on the peri-infarct region. (A–D) Representative images of beclin signal (red) and TUNEL-positive cells (green) at 24 h after ischemia in nondiabetic stroke mice (A and B) and diabetic stroke mice (C, D). B and D are higher magnification of the framed region in A and C, respectively. Arrowheads point to beclin-positive cells. E. Quantified data showed significantly increased beclin signals in the penumbra region at 12 and 24 h postischemia in diabetic animals compared with regular controls. N = 5 per group at each time point. * $P < 0.05$ vs. nondiabetic stroke controls.

and cells colabeled with TUNEL staining was significantly elevated in diabetic stroke mice compared with nondiabetic stroke controls 24 h after ischemia (Figure 2B–D).

The conversion from LC3-I to LC3-II occurs in autophagy, while the LC3-II level is regarded more reliable in autophagy measurement [32,33]. LC3-II was thus detected using Western blotting in penumbra tissues of the ischemic brain. No difference was seen in the basal level of LC3-II between diabetic and nondiabetic mice (data not shown). In stroke animals, LC3-II levels significantly increased 24 h after ischemia in both groups (Figure 2E). Even more LC3 conversion was detected in diabetic stroke mice compared with nondiabetic ischemic controls (Figure 2F). As expected, the augmented LC3-II conversion could be largely prevented by the autophagy inhibitor 3-MA (Figure 2F).

Increased Autophagosome Flux in Diabetic Stroke Mice

As autophagy is a dynamic process, the increased number of autophagosomes could result from either increased autophagic activity (autophagic flux) or decreased degradation of autophagosomes [21]. To distinguish these possibilities, levels of the lysosomal protease cathepsin D and the autophagy-specific substrate p62 were measured in the postischemic brain [21,34]. At 24 h postischemia, immunostaining revealed cells with cathepsin D-positive dots in the peri-infarct region of both diabetic and nondiabetic stroke brain sections (Figure 3B,C). At high magnification, double staining showed strong autophagosomal LC3 labeling and lysosomal cathepsin D labeling in the same cells (Figure 3A–C).

In Western blot analysis, focal cerebral ischemia induced significant decreases in the p62 level. In diabetic stroke mice, the reduction was much greater compared with nondiabetic stroke animals (Figure 3D). Thus, increased LC3 signaling and decreased p62 expression support an upregulation of autophagic flux in diabetic stroke mice.

Increased Ischemic Brain Damage and Neuroprotective Effect of Autophagy Inhibition in Diabetic Stroke Mice

Diabetic stroke mice showed significantly larger brain infarct volume: the infarct volume measured using TTC staining was 28% larger than that in age-matched nondiabetic stroke animals (Figure 4A,B). Diabetic stroke mice showed an increased percentage of TUNEL-positive cells in the penumbra region (0.45 ± 0.02 vs. 0.37 ± 0.01 , in diabetic and nondiabetic mice, respectively, $n = 5$ and 15 for nondiabetic and diabetic mice, respectively, $P < 0.05$) 24 h after stroke (Figure 4C–F).

As we observed augmented autophagic activity in the diabetic stroke brain, we tested the hypothesis that the increased autophagy contributed to the more severe brain damage. Intraventricular injection of 3-MA, at a dosage that could block LC3-II conversion (Figure 2F), was applied to diabetic stroke animals. 3-MA reduced infarct volume both in regular and diabetic mice measured using TTC staining (Figure 4B). In a closer examination at the cellular level, a significant reduction of TUNEL-positive cells was seen with 3-MA 24 h after stroke in nondiabetic stroke mice and diabetic stroke mice (Figure 4G).

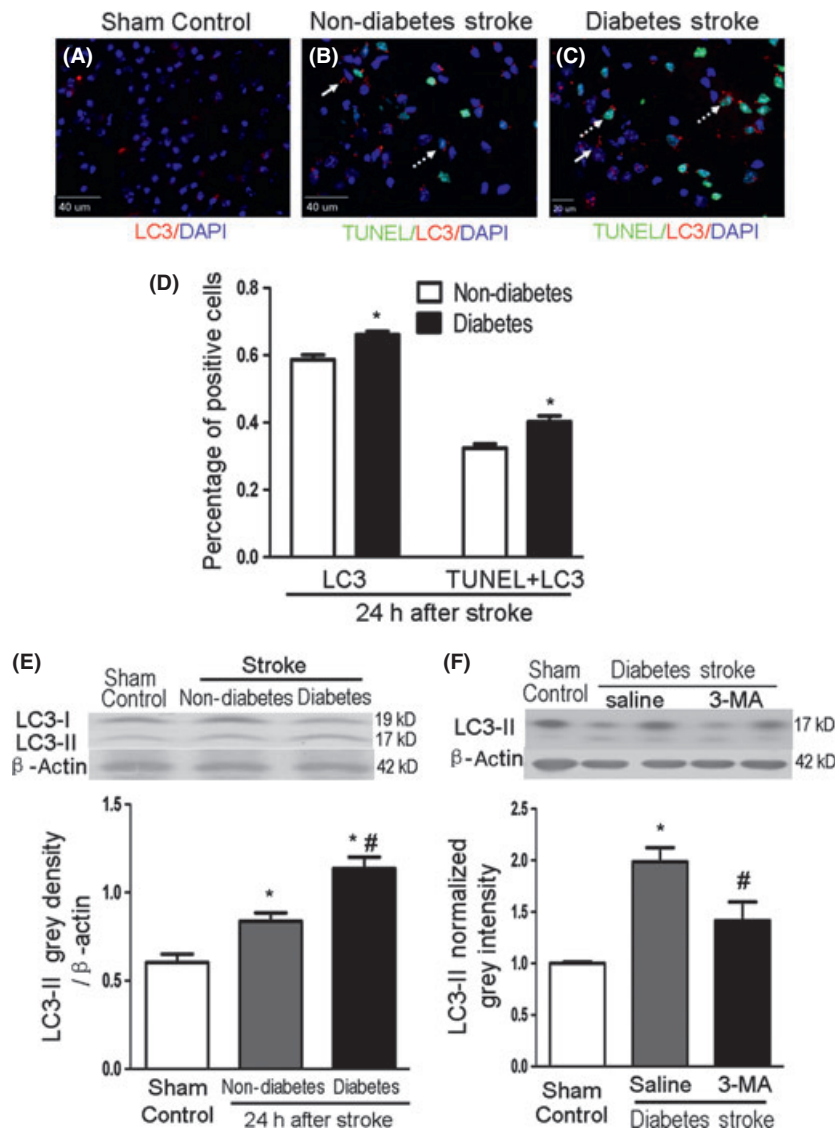


Figure 2 Increased autophagic cell death in the diabetic stroke brain. Immunohistochemical staining and Western blotting were applied to specifically detect autophagy-associated signals in sham controls and after ischemic stroke. **(A–D)** The LC3 staining in sham controls are diffuse red signals as shown in image **A**. The bright red punctuate structures around nuclei (DAPI: blue) in images **B** and **C** are the LC3 signal representing autophagosomes 24 h after ischemic insult. The arrows indicate the cells with increased autophagosome; dashed arrows showed cells that are positive for both LC3 and TUNEL staining [54]. **(D)** Quantification data show significant increases in LC3-positive cells as well as LC3 and TUNEL double-positive cells in the penumbra region 24 h after ischemia in diabetic mice. $N = 5$ per group. * $P < 0.05$ vs. nondiabetic stroke controls. **(E)** LC3-II conversion assessed using Western blotting in sham control and the postischemic brain. Upper panel is representative immunoblot of LC3 in extracts of the penumbra region. Lower panel shows quantification of the LC3-II band intensity ratio compared with loading controls. At 24 h after ischemia, the level of LC3-II in both nondiabetic control and diabetic animals was elevated, but the increase was much greater in the diabetic brain. $N = 2$ for sham control, $n = 5$ for nondiabetic stroke and diabetic stroke mice, respectively. **(F)** In diabetic stroke mice, the LC3-II expression was about doubled from the sham control level. 3-MA treatment significantly brought down the LC3-II conversation. $N = 3$ for sham group, $n = 4$ for diabetes stroke saline or 3-MA group. One-way ANOVA followed by Bonferroni selective comparisons was performed for analyzing the level of LC3 between nondiabetic stroke and sham animals. * $P < 0.05$ vs. sham control, # $P < 0.05$ vs. nondiabetic stroke in E or saline control in F.

The tight junction protein occludin is a marker of interendothelial clefts and an important indicator of the integrity and paracellular permeability of the blood–brain barrier (BBB) [35,36]. Diabetes had no effect on occludin expression in sham controls (data not shown). Compared with sham controls, occludin levels were significantly decreased 24 hrs after ischemia in both diabetic and normo-

glycemic groups. The decrease, however, was significantly greater in diabetic stroke animals (Figure 5A–E). 3-MA treatment soon after stroke led to noticeable preservation of occludin levels in nondiabetic stroke mice; the effect on occludin expression in diabetic stroke mice, however, was not significant in immunostaining experiments (Figure 5E). As the immunohistochemical method

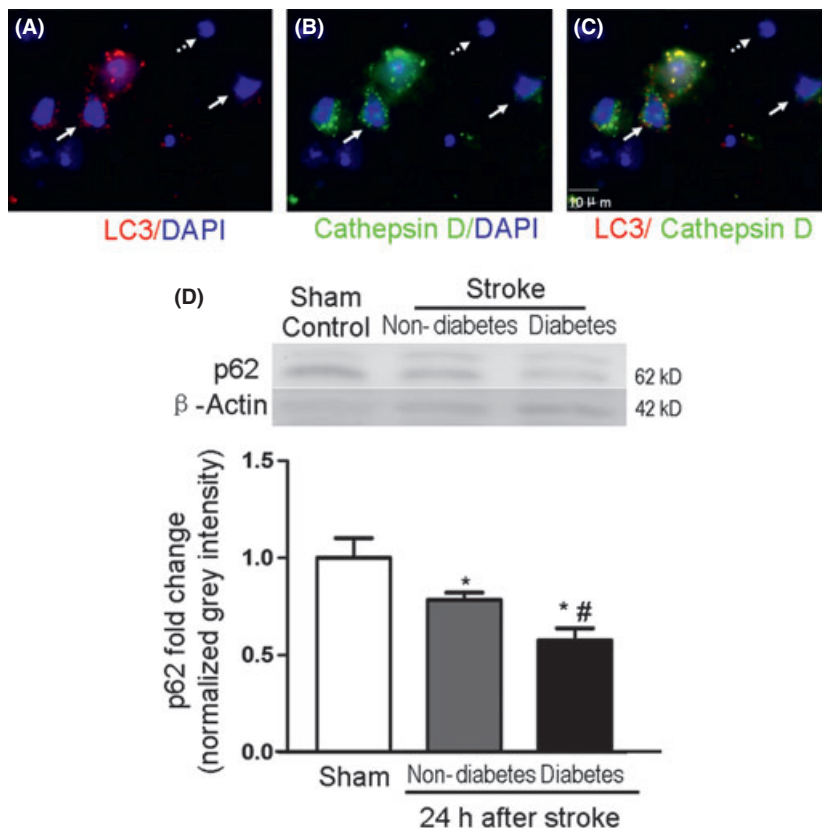


Figure 3 Increased autophagic flux in diabetic stroke mice. Immunohistochemical staining or Western blotting of autophagic flux signals in sham control and stroke animals. (A–C) Representative images showing colocalization of autophagosomal marker (LC3, red) and lysosomal marker (cathepsin D, green) within the same cells (DAPI: blue) in the penumbral cortex of diabetes mice. Arrows show cells double-labeled with LC3 and cathepsin D. Dashed arrow shows a cell which is negative for both signals. (D) Upper panel: Representative immunoblot of p62 in extracts of ischemic penumbra cortex at 24 h postischemia. Lower panel: Quantification of the p62 band intensity expressed as a percentage of sham p62. There was significantly decreased expression level of p62 in the penumbra cortex of both nondiabetic and diabetic stroke animals at 24 h postischemia. N = 2 for sham, n = 5 for nondiabetic and diabetic stroke mice, respectively. One-way ANOVA followed by Bonferroni selective comparisons was carried out for the analysis. * $P < 0.05$ vs. sham control, # $P < 0.05$ vs. nondiabetic stroke.

surveys a limited region of the ischemic brain, we then assessed the occludin expression in the peri-infarct cortex using Western blot analysis and identified that 3-MA treatment significantly increased the occludin protein level in diabetic stroke mice comparing with saline-treated diabetic mice (Figure 5F).

Effects of 3-MA Treatment on Apoptotic Cell Death Pathways

The interaction between apoptotic and autophagic pathways has been proven both in vitro and in nondiabetic cerebral ischemic animals [10,37]. We tested whether this cross-talk exists in a diabetic condition. In Western blotting assays using the antibody against cleaved caspase-3, both nondiabetic and diabetic stroke mice showed significant caspase-3 activation in peri-infarct region (Figure 6A). 3-MA treatment significantly suppressed the caspase-3 activation by about 50% (Figure 6A). In diabetic stroke mice, the cerebral ischemia did not change the level of antiapoptotic protein Bcl-2 24 h postischemia, while 3-MA treatment significantly doubled the expression of Bcl-2 in the diabetic stroke brain (Figure 6B). These experiments focused on the diabetic condition support the idea that apoptotic cell death contributed significantly to ischemic brain injury.

Sensorimotor Functional Deficit after Ischemic Stroke and Effect of 3-MA

In neurological functional assays, worse deficits were seen with diabetic stroke mice compared with nondiabetic stroke mice. In

adhesive-removal test, both nondiabetic and diabetic stroke mice took significantly more time to detect and remove sticky dots attached to their ischemia-affected left paws (Figure 7A,B). Stroke mice in both groups received the 3-MA treatment (30 ng, i.c.v. soon after ischemia) showed improvements in the functional assessment. 3-MA-treated diabetic stroke mice was significantly faster in detecting the sticky dot (shorter latency), although the reduction in removal time was not significant (Figure 7A,B). The 3-MA treatment in nondiabetic stroke animals did not reach to statistical significance in these experiments (Figure 7A,B).

Discussion

The present investigation demonstrates that ischemic brain damage is exacerbated in STZ/NA-induced diabetic mice. The exaggerated brain damage occurs concurrently with upregulated autophagic activity in the ischemic brain. We provide novel evidence that not only autophagosome formation but also autophagic flux is augmented in diabetic stroke mice. Blocking the postischemic autophagy using the autophagy inhibitor 3-MA prevents the excessive ischemic brain damage in diabetic mice as well as shows improvements in functional recovery after ischemic stroke.

In the STZ/NA-induced diabetic mouse model, we confirmed that these mice developed nonobese diabetic symptoms characterized by stable hyperglycemia (200–300 mg/dL), hypoinsulinemia (68% reduction), and growth impairment after STZ treatment [26,38]. Due to the partial protection of NA against the β -cell cytotoxic effect of STZ, these diabetic mice showed better overall well-being and lower mortality rates when subjected to the cere-

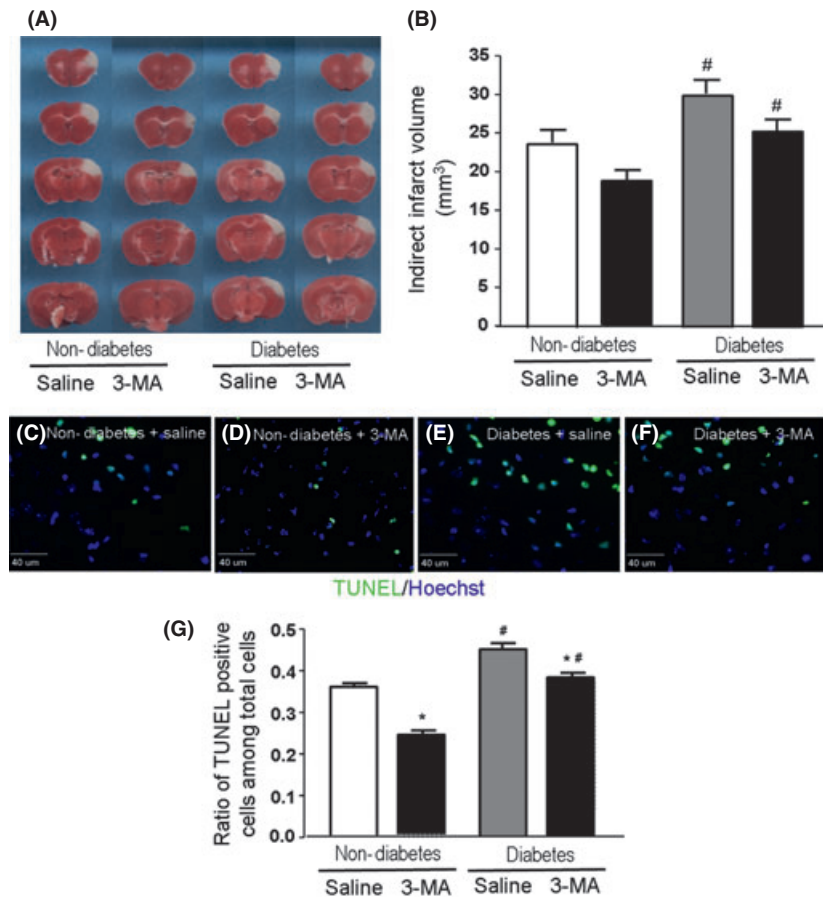


Figure 4 Protective effect of autophagy inhibition with 3-MA in the diabetic ischemic brain. Cerebra ischemia-induced brain infarct formation and cell death were measured 24 h after the onset of MCA occlusion using TTC and TUNEL staining, respectively. Autophagy was blocked using i.c.v. injection of 3-MA immediately after ischemia. **(A)** TTC staining images of infarct area (white) in nondiabetic stroke control, diabetic stroke mice received saline vehicle treatment and 3-MA treatment. **(B)** Quantified TTC staining measurement of infarct volume calculated using the indirect method. Diabetic mice showed significantly larger infarct volume compared with nondiabetic stroke mice ($n = 8$ and 11 , respectively). 3-MA treatment showed a trend of reducing the infarct volume ($n = 10$, $P = 0.14$). The 3-MA effect become significant when direct measurement of infarct volume was applied (data not shown), indicating that 3-MA had an inhibitory action on brain edema. **(C–F)** Immunofluorescent images of all nuclei (Hoechst, blue) and TUNEL-positive (green) cells in the penumbra region of the nondiabetic and diabetic stroke brain with and without 3-MA. **(G)** Cell counting results from the immunostaining assay. Diabetes significantly increased the percentage of TUNEL-positive cells ($n = 5$ and 15 for nondiabetic and diabetic mice, respectively). 3-MA treatment soon after ischemia ($n = 12$) significantly attenuated the percentage of TUNEL-positive cells. $^*P < 0.05$ versus saline controls, $^{\#}P < 0.05$ versus non-diabetes saline group.

bral ischemic insult compared with animals rendered diabetic by STZ alone. This type of diabetic model is closer to type 2 diabetes with respect to β -cell dysfunction, diminished insulin-to-glucose ratio, and calorie-controlled high-fat diet leading to insulin resistance [38]. Upon focal cerebral ischemia after 2 months of hyperglycemia, these diabetic animals exhibited larger infarct volume, enhanced cell death ratio in the penumbral region, more severe BBB disruptions and worse functional deficits compared with normoglycemic controls. As it is well known that ischemic injury is exaggerated with hyperglycemia [39], we assume the increased damage is closely related to the hyperglycemia-associated oxidative stress, vascular inflammation and tissue acidosis as well as impaired cellular metabolism [40–42].

Autophagy occurs at basal levels in most tissues as part of homeostatic functions and is involved in development, differentia-

tion, and tissue remodeling [43,44]. Autophagy plays a double-edged role in certain diseases, including cancer, liver disease, muscular disorders, β -cell mass loss in diabetes, and neurodegenerative diseases. Despite the physiological role of cellular protection, autophagic activities in these disease states may contribute to cell damage depending on the cellular milieu [9,13,43]. Previous evidence indicates that autophagic cell death is a potential contributor to ischemia-induced neuronal cell death in nondiabetic stroke animals [10,18–23]. Consistent with the general idea that autophagy is an insult to neuronal cells, autophagy has been shown to generate a preconditioning effect against ischemic damage [45,46]. Our present investigation suggests that increased autophagy flux plays a role in exaggerated cell death in the diabetic ischemic brain. This is in line with a previous report that autophagy increases after a global ischemic insult in diabetic mice [17].

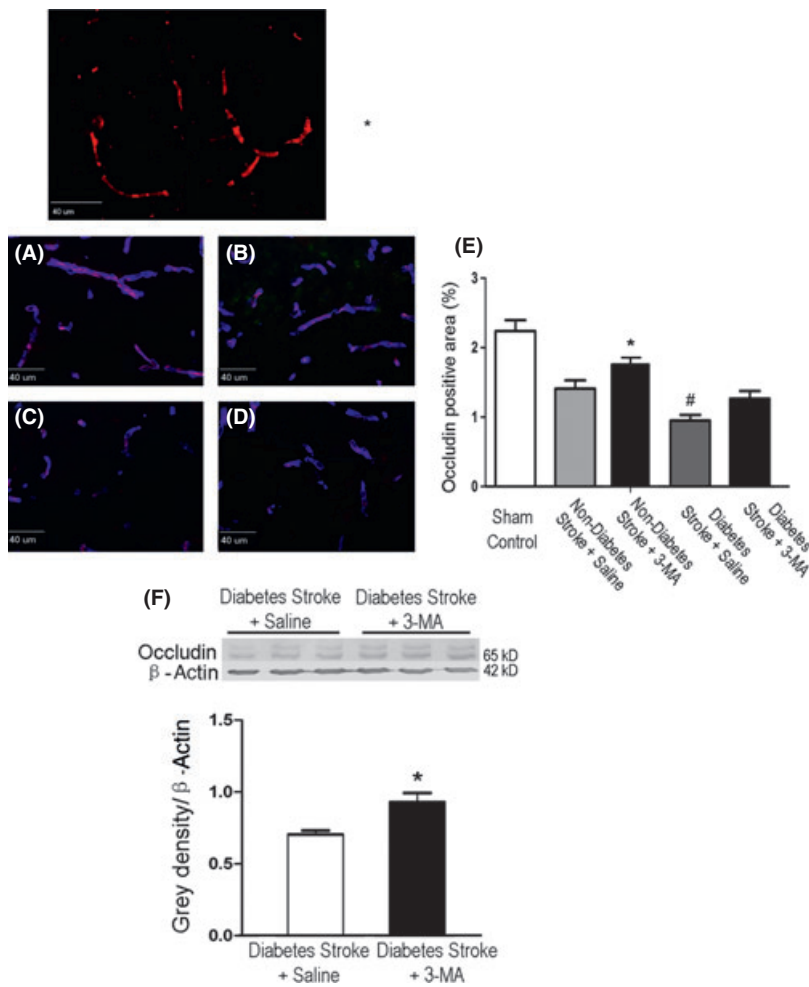


Figure 5 Effect of inhibiting autophagy on tight junction disruption. Immunohistochemical staining and Western blotting were used to detect the expression level of the tight junction marker occludin in the penumbra of normal and stroke animals. (A–D) Immunostaining images of occludin (red) and collagen IV (blue) in sham control animals (A), nondiabetic stroke mice (B), diabetic stroke mice (C), and diabetic stroke animals with 3-MA treatment. (E) Image data were quantified by the area percentage based on fluorescence density. Stroke markedly decreased the occludin expression level in the saline groups of both nondiabetic and diabetic mice. 3-MA treatment significantly attenuated the occludin decrease. $N = 4-5$ in each group; * $P < 0.05$ vs. sham control, # $P < 0.05$ vs. nondiabetic stroke control. (F) Western blot analysis of occludin protein levels in the brain from diabetic stroke animals. Upper panel: representative immunoblots. Lower panel: Quantification of occludin band intensities expressed as ratio compared with β -actin loading controls. 3-MA treatment preserved occluding levels relative to stroke saline group of diabetic mice. $N = 5$ in each group, * $P < 0.05$ vs. diabetic stroke plus saline.

During autophagy process, the membrane-bound structure autophagosome is formed to sequester cytoplasm. The autophagosome fuses with a lysosome, where it is degraded and the macromolecules recycled [43]. We showed that there is an upregulation of LC3-II conjugate, a marker for autophagosomes, assessed by both Western blotting and immunostaining in diabetic stroke mice comparing with age-matched nondiabetic stroke mice. Double labeling showed that the increased number of autophagosomes colocalized with the upregulated lysosomal marker cathepsin D in the same cells. Further evidence for upregulated autophagic flux came from the assay on the level of p62, a specific substrate that is preferentially degraded by autophagy. This assay showed greater decreases of p62 in diabetic stroke animals compared with nondiabetic controls, which is consistent with augmented autophagic activities. These results provide evidence that there is an increase in autophagic flux, not just an increase in autophagosomes formation in diabetic stroke mice. To further determine the role of the upregulated autophagic flux in the pathology of diabetic stroke, we tested the effects of the autophagy inhibitor 3-MA. Our results showed that 3-MA prevented exaggerated brain damage in diabetic mice and lowered the injury to the level of nondiabetic stroke mice. 3-MA also showed functional benefits in diabetic stroke animals. These data indicate that the increased autophagic

flux contributes to the exacerbated ischemic brain damage in diabetic mice.

There are limitations that can be identified in the experiment using 3-MA. 3-MA is a PI3-kinase inhibitor (both class I and class III) and has been widely used as a pharmacological inhibitor in autophagy studies. However, 3-MA is not autophagy specific [21,47]. 3-MA acts on other kinases and affects other cellular process such as lysosomal acidification and the mitochondrial permeability transition [21]. In the present investigation, we did not solely rely on the pharmacological tool for the demonstration of the involvement of autophagy. The increased expression level of LC3 and decreased level of P62 in diabetic stroke mice and the colocalization of LC3 and cathepsin D in the same cells agree that autophagic flux indeed increases in the diabetic mice. Knocking down or deleting specific autophagy genes such as Atg7 and combined therapy with autophagy and apoptosis inhibitors may provide more specific evidence in further experiments.

It has been shown that autophagy can either directly execute cell death in Bax/Bak double knockout mice or alter the dynamics of death through interactions with apoptosis [43,48,49]. Apoptosis and autophagy pathways may act synergistically or counter each other by sharing many of the same molecular regulators, such as Bcl-2 family proteins and sphingo-lipid metabolic pathways

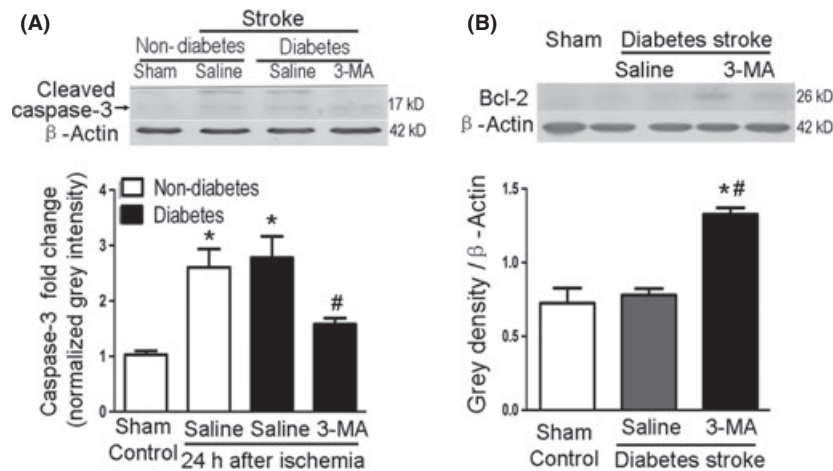


Figure 6 Effects of 3-MA on caspase-3 activation and the expression level of Bcl-2 in the diabetic stroke brain. Western blot was performed 24 hr after the onset of MCA occlusion. **(A)** Expression of cleaved caspase-3 in the penumbra region. Upper panel: representative immunoblots. Lower panel: Quantification of cleaved caspase-3 band intensities expressed as a fold change from the sham level of cleaved caspase-3. Caspase-3 activity was significantly increased both non-diabetic and diabetic stroke mice penumbra. 3-MA treatment significantly suppressed the caspase-3 activation by about 50% in diabetic stroke mice. **(B)** Upper panel: representative immunoblots of Bcl-2 expression level in the extracts of ischemic penumbra cortex. Lower panel: Quantification of Bcl-2 band intensities normalized to actin loading controls. In diabetic stroke mice, the cerebral ischemia did not change the Bcl-2 level, while 3-MA treatment significantly doubled the expression of Bcl-2 in the diabetic stroke brain. N = 5 in each group, **P* < 0.05 vs. sham controls, #*P* < 0.05 vs. diabetic stroke plus saline.

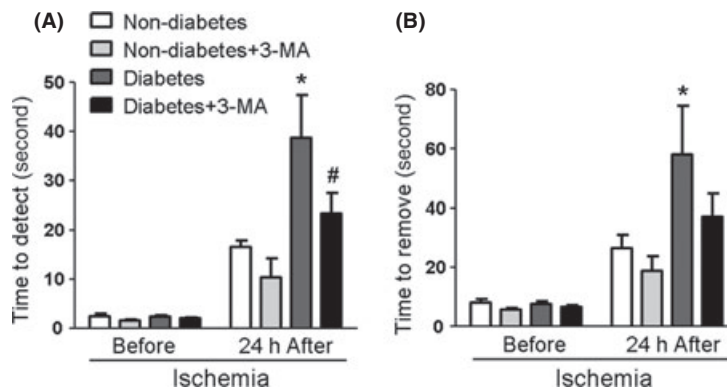


Figure 7 Functional benefits of 3-MA treatment in diabetic stroke mice. Sensorimotor functional activity was assessed using the removal test performed 24 h after stroke. **(A)** Measurement of time to detect the attached dot on the affected paw corresponding to the ischemic sensorimotor cortex. There were no differences among groups before stroke. Functional deficit of prolonged detection time was seen 24 h after stroke in both nondiabetic and diabetic animals. 3-MA showed a strong trend of shortening the detecting time (*P* = 0.09) in nondiabetic stroke mice. The shortening in 3-MA-treated mice was statistically significant. **(B)** Measurement of time to remove the attached dot. All animals showed similar removal times before stroke, stroke caused significant delay in the removal time. Between nondiabetic and diabetic groups, diabetic stroke mice took much longer time to remove the sticky dot from their pawns. This functional deficit was largely corrected by 3-MA treatment. The correction by 3-MA in nondiabetic mice was not significant. N = 7 in control groups, n = 11 for nondiabetic stroke groups, n = 8 and 6 for diabetic with and without 3-MA treatments. **P* < 0.05 vs. nonstroke controls (before stroke), #*P* < 0.05 vs. diabetic stroke control.

[9,37,50]. The cross-talk between these two pathways has been proven both in vitro and in nondiabetic cerebral ischemic animals [10,37]. It remains to be verified whether the postischemia autophagic activity damages the cells directly or through interactions with the apoptotic cell death pathway. Our data suggested that autophagy and apoptosis seemed to be linked in diabetic cerebral ischemic animals, because inhibiting autophagy with 3-MA markedly attenuates caspase-3 activation and augments the antiapoptotic protein Bcl-2 expression. The latter is the founding member of the Bcl-2 family of apoptosis regulators [51] and is reported to

be participate in the inhibition of autophagy through the interaction of Bcl-2/Bcl-XL with Beclin 1 [52]. This observation further suggests possible crosstalk between autophagy and apoptosis after focal cerebral ischemia in diabetic mice. The markedly increased antiapoptotic gene Bcl-2 by 3-MA is an interesting observation, which may contribute partially to the neuroprotective effect of 3-MA in the ischemic brain at the time when PI3K kinases are inhibited.

In our study, over 80% of TUNEL-positive cells in the penumbra region showed positive staining with autophagic markers such

as LC3. Given the fact that cell death is often accompanied by features of autophagy, we cannot conclude that this majority of TUN-EL/LC3 double-positive cells undergo cell death through a pure autophagy pathway [53]. In previous investigations, we showed that ischemia-induced neuronal damage is a mixed form of cell death, including concurrent necrotic and apoptotic features in the same cells [7]. This hybrid or mixed cell death can be demonstrated in vitro under conditions such as oxygen glucose deprivation and Na^+/K^+ -ATPase failure [28]. More evidence implicates that the hybrid cell death is a common form of cell death after ischemia in vivo when the insult simultaneously triggers multiple cell death pathways [7,37]. The present investigation provides further evidence that autophagy is one of the contributors to the hybrid cell death mechanism in the ischemic brain.

We recognize that identification of autophagy in different cell populations will provide additional information for the cell death mechanism in different cells such as glial and endothelial cells. In our cell counting assay on double staining with LC3-II and NeuN, over 90% LC3-II-positive cells were NeuN positive. On the other hand, ischemia-induced BBB disruption is worse in diabetic mice than in nondiabetic mice, suggesting exacerbated injury to vascular endothelial cells. As 3-MA attenuates the BBB damage, autophagy may occur in endothelial cells. A further investigation will be needed to focus on the role of autophagy in endothelial cells, neurovascular unit and BBB damage in nondiabetic and diabetic mice.

In conclusion, we here report novel evidence for the involvement of upregulated autophagic activity in mediating exaggerated brain damage in diabetic mice after focal cerebral ischemia. The excessive autophagy in diabetic stroke mice could result from diabetes-related factors like hyperglycemia, insulin deficiency, and other related metabolic defects. Further studies will be needed to explore the underlying mechanism. Collectively, these results suggest that autophagy pathway is associated with worsened tissue damage in diabetic stroke. The involvement of autophagy-mediated neuronal and vascular cell injury merits further attention in the cell death mechanism of diabetic stroke and provides a potential new target for the treatment of ischemic stroke in patients with diabetes.

Acknowledgments

This work was supported by NIH grants NS057255 (LW), NS075338 (LW), NS062097 (LW), NS0458710 (SPY), and an AHA Established Investigator Award (LW). This work was also supported by the NIH grant C06 RR015455 from the Extramural Research Facilities Program of the National Center for Research Resources.

Conflict of Interest

The authors declare no conflict of interest.

References

- Moskowitz MA, Lo EH, Iadecola C. The science of stroke: mechanisms in search of treatments. *Neuron* 2010;**67**:181–198.
- Lawes CM, Parag V, Bennett DA, et al. Blood glucose and risk of cardiovascular disease in the Asia Pacific region. *Diabetes Care* 2004;**27**:2836–2842.
- Gisselsson L, Smith ML, Siesjo BK. Hyperglycemia and focal brain ischemia. *J Cereb Blood Flow Metab* 1999;**19**:288–297.
- Muranyi M, Fujioka M, He Q, et al. Diabetes activates cell death pathway after transient focal cerebral ischemia. *Diabetes* 2003;**52**:481–486.
- Arboix A, Rivas A, Garcia-Eroles L, et al. Cerebral infarction in diabetes: clinical pattern, stroke subtypes, and predictors of in-hospital mortality. *BMC Neurol* 2005;**5**:9.
- Bruno A, Liebeskind D, Hao Q, et al. Diabetes mellitus, acute hyperglycemia, and ischemic stroke. *Curr Treat Options Neurol* 2010;**12**:492–503.
- Wei L, Ying DJ, Cui L, et al. Necrosis, apoptosis and hybrid death in the cortex and thalamus after barrel cortex ischemia in rats. *Brain Res* 2004;**1022**:54–61.
- Biessels GJ, van der Heide LP, Kamal A, et al. Ageing and diabetes: implications for brain function. *Eur J Pharmacol* 2002;**441**:1–14.
- Eisenberg-Lerner A, Bialik S, Simon HU, et al. Life and death partners: apoptosis, autophagy and the cross-talk between them. *Cell Death Differ* 2009;**16**:966–975.
- Puyal J, Vaslin A, Mottier V, et al. Postischemic treatment of neonatal cerebral ischemia should target autophagy. *Ann Neurol* 2009;**66**:378–389.
- Wang P, Miao CY. Autophagy in the disorders of central nervous system: vital and/or fatal? *CNS Neurosci Ther* 2012;**18**:955–956.
- Wei K, Wang P, Miao CY. A double-edged sword with therapeutic potential: an updated role of autophagy in ischemic cerebral injury. *CNS Neurosci Ther* 2012;**18**:879–886.
- Chen ZF, Li YB, Han JY, et al. The double-edged effect of autophagy in pancreatic beta cells and diabetes. *Autophagy* 2011;**7**:12–16.
- Kaniuk NA, Kiraly M, Bates H, et al. Ubiquitinated-protein aggregates form in pancreatic beta-cells during diabetes-induced oxidative stress and are regulated by autophagy. *Diabetes* 2007;**56**:930–939.
- Tanaka Y, Kume S, Kitada M, et al. Autophagy as a therapeutic target in diabetic nephropathy. *Exp Diabetes Res* 2012;**2012**:628978.
- Gonzalez CD, Lee MS, Marchetti P, et al. The emerging role of autophagy in the pathophysiology of diabetes mellitus. *Autophagy* 2011;**7**:2–11.
- Zhang T, Yan W, Li Q, et al. 3-n-Butylphthalide (NBP) attenuated neuronal autophagy and amyloid-beta expression in diabetic mice subjected to brain ischemia. *Neurol Res* 2011;**33**:396–404.
- Bouet V, Bouluard M, Toutain J, et al. The adhesive removal test: a sensitive method to assess sensorimotor deficits in mice. *Nat Protoc* 2009;**4**:1560–1564.
- He S, Wang C, Dong H, et al. Immune-related GTPase M (IRGM1) regulates neuronal autophagy in a mouse model of stroke. *Autophagy* 2012;**8**:1621–1627.
- Liu C, Gao Y, Barrett J, et al. Autophagy and protein aggregation after brain ischemia. *J Neurochem* 2010;**115**:68–78.
- Mizushima N, Yoshimori T, Levine B. Methods in mammalian autophagy research. *Cell* 2010;**140**:313–326.
- Wen YD, Sheng R, Zhang LS, et al. Neuronal injury in rat model of permanent focal cerebral ischemia is associated with activation of autophagic and lysosomal pathways. *Autophagy* 2008;**4**:762–769.
- Grishchuk Y, Ginet V, Truttmann AC, et al. Beclin 1-independent autophagy contributes to apoptosis in cortical neurons. *Autophagy* 2011;**7**:1115–1131.
- Zhang T, Liu X, Li Q, et al. Exacerbation of ischemia-induced amyloid-beta generation by diabetes is associated with autophagy activation in mice brain. *Neurosci Lett* 2010;**479**:215–220.
- Masiello P, Broca C, Gross R, et al. Experimental NIDDM: development of a new model in adult rats administered streptozotocin and nicotinamide. *Diabetes* 1998;**47**:224–229.
- Novelli M, D'Aleo V, Lupi R, et al. Reduction of oxidative stress by a new low-molecular-weight antioxidant improves metabolic alterations in a nonobese mouse diabetes model. *Pancreas* 2007;**35**:e10–e17.
- Whitaker VR, Cui L, Miller S, et al. Whisker stimulation enhances angiogenesis in the barrel cortex following focal ischemia in mice. *J Cereb Blood Flow Metab* 2007;**27**:57–68.
- Xiao AY, Wei L, Xia S, et al. Ionic mechanism of ouabain-induced concurrent apoptosis and necrosis in individual cultured cortical neurons. *J Neurosci* 2002;**22**:1350–1362.
- Kihara A, Kabeya Y, Ohsumi Y, et al. Beclin-phosphatidylinositol 3-kinase complex functions at the trans-Golgi network. *EMBO Rep* 2001;**2**:330–335.
- Rangaraju S, Verrier JD, Madorsky I, et al. Rapamycin activates autophagy and improves myelination in explant cultures from neuropathic mice. *J Neurosci* 2010;**30**:11388–11397.
- Kabeya Y, Mizushima N, Ueno T, et al. LC3, a mammalian homologue of yeast Apg8p, is localized in autophagosome membranes after processing. *EMBO J* 2000;**19**:5720–5728.
- Mizushima N, Yoshimori T. How to interpret LC3 immunoblotting. *Autophagy* 2007;**3**:542–545.
- Tanida I, Ueno T, Kominami E. LC3 and Autophagy. *Methods Mol Biol* 2008;**445**:77–88.

34. Bjorkoy G, Lamark T, Brech A, et al. p62/SQSTM1 forms protein aggregates degraded by autophagy and has a protective effect on huntingtin-induced cell death. *J Cell Biol* 2005;**171**:603–614.
35. Liu W, Hendren J, Qin XJ, et al. Normobaric hyperoxia attenuates early blood-brain barrier disruption by inhibiting MMP-9-mediated occludin degradation in focal cerebral ischemia. *J Neurochem* 2009;**108**:811–820.
36. Tavelin S, Hashimoto K, Malkinson J, et al. A new principle for tight junction modulation based on occludin peptides. *Mol Pharmacol* 2003;**64**:1530–1540.
37. Wei L, Han BH, Li Y, et al. Cell death mechanism and protective effect of erythropoietin after focal ischemia in the whisker-barrel cortex of neonatal rats. *J Pharmacol Exp Ther* 2006;**317**:109–116.
38. Nakamura T, Terajima T, Ogata T, et al. Establishment and pathophysiological characterization of type 2 diabetic mouse model produced by streptozotocin and nicotinamide. *Biol Pharm Bull* 2006;**29**:1167–1174.
39. Harada S, Fujita-Hamabe W, Tokuyama S. Ischemic stroke and glucose intolerance: a review of the evidence and exploration of novel therapeutic targets. *J Pharmacol Sci* 2012;**118**:1–13.
40. Folbergrova J, Memezawa H, Smith ML, et al. Focal and perifocal changes in tissue energy state during middle cerebral artery occlusion in normo- and hyperglycemic rats. *J Cereb Blood Flow Metab* 1992;**12**:25–33.
41. Widmer H, Abiko H, Faden AI, et al. Effects of hyperglycemia on the time course of changes in energy metabolism and pH during global cerebral ischemia and reperfusion in rats: correlation of 1H and 31P NMR spectroscopy with fatty acid and excitatory amino acid levels. *J Cereb Blood Flow Metab* 1992;**12**:456–468.
42. Yan J, Feng Z, Liu J, et al. Enhanced autophagy plays a cardinal role in mitochondrial dysfunction in type 2 diabetic Goto-Kakizaki (GK) rats: ameliorating effects of (-)-epigallocatechin-3-gallate. *J Nutr Biochem* 2012;**23**:716–724.
43. Shintani T, Klionsky DJ. Autophagy in health and disease: a double-edged sword. *Science* 2004;**306**:990–995.
44. Levine B, Klionsky DJ. Development by self-digestion: molecular mechanisms and biological functions of autophagy. *Dev Cell* 2004;**6**:463–477.
45. Wang P, Guan YF, Du H, et al. Induction of autophagy contributes to the neuroprotection of nicotinamide phosphoribosyltransferase in cerebral ischemia. *Autophagy* 2012;**8**:77–87.
46. Sheng R, Liu XQ, Zhang LS, et al. Autophagy regulates endoplasmic reticulum stress in ischemic preconditioning. *Autophagy* 2012;**8**:310–325.
47. Petiot A, Ogier-Denis E, Blommaert EF, et al. Distinct classes of phosphatidylinositol 3'-kinases are involved in signaling pathways that control macroautophagy in HT-29 cells. *J Biol Chem* 2000;**275**:992–998.
48. Yu L, Alva A, Su H, et al. Regulation of an ATG7-beclin 1 program of autophagic cell death by caspase-8. *Science* 2004;**304**:1500–1502.
49. Shimizu S, Kanaseki T, Mizushima N, et al. Role of Bcl-2 family proteins in a non-apoptotic programmed cell death dependent on autophagy genes. *Nat Cell Biol* 2004;**6**:1221–1228.
50. Pattingre S, Tassa A, Qu X, et al. Bcl-2 antiapoptotic proteins inhibit Beclin 1-dependent autophagy. *Cell* 2005;**122**:927–939.
51. Zhang T, Jia W, Sun X. 3-n-Butylphthalide (NBP) reduces apoptosis and enhances vascular endothelial growth factor (VEGF) up-regulation in diabetic rats. *Neurol Res* 2010;**32**:390–396.
52. Levine B, Sinha S, Kroemer G. Bcl-2 family members: dual regulators of apoptosis and autophagy. *Autophagy* 2008;**4**:600–606.
53. Denton D, Nicolson S, Kumar S. Cell death by autophagy: facts and apparent artefacts. *Cell Death Differ* 2012;**19**:87–95.
54. Galluzzi L, Vitale I, Abrams JM, et al. Molecular definitions of cell death subroutines: recommendations of the Nomenclature Committee on Cell Death 2012. *Cell Death Differ* 2012;**19**:107–120.